204. Coenzyme F430 from Methanogenic Bacteria: Oxidation of F430 Pentamethyl Ester to the Ni(III) Form

by **Bernhard Jaun**

Laboratorium für organische Chemie, Eidgenössische Technische Hochschule, Universitätstr. 16, CH–8092 Zürich

(21.IX.90)

F430M, the pentamethyl ester of coenzyme F430, can be oxidized reversibly by one electron. The oxidation potential has been determined, and the electrolytically prepared oxidation product was characterized by its UV/VIS and ESR spectrum. The strongly anisotropic and nearly axial ESR spectrum is consistent with a S = ½ species with the unpaired-electron spin density predominantly in a d_{z^2}-type orbital of the central nickel ion. The properties of Ni(III)F430M are discussed in the context of two hypothetical mechanisms for the catalytic role of coenzyme F430 in methyl coenzyme M reductase, which catalyses the last step of methane formation in methanogenic bacteria.

1. Introduction. – Factor F430 [1], the hydrocorphinoid nickel complex **1**, is the prosthetic group of methyl coenzyme M reductase [2] which catalyses the last step of CH_4 formation in methanogenic bacteria according to *Scheme 1* [3].

While recent biophysical evidence points to a change of the redox state of coenzyme F430 during the catalytic cycle [5], the specific mechanism by which the enzyme catalyses this process is still unknown. One conceivable way of activation of the C–S bond in methyl coenzyme M is the addition of a thiyl radical to the thioether, followed by transfer of a Me group from the sulfuranyl intermediate to the Ni center of coenzyme F430.

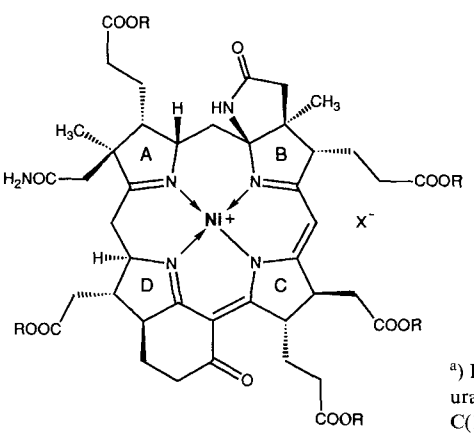

1 Coenzyme F430 (R = H)[a])
2 F430M (R = CH_3, X = ClO_4)[a])

[a]) Based on recent results [4], the configuration at centers C(17), C(18), and C(19) is as shown here and, for C(18) and C(19), opposite to the original tentative assignment [1c].

Scheme 1

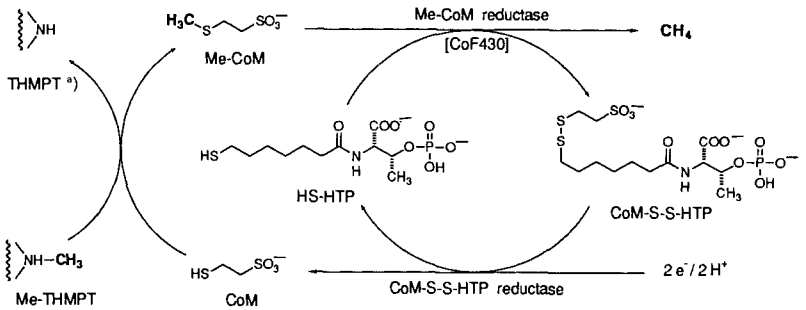

a) THMPT = tetrahydro-methanopterin [6].

Evidence for the existence of sulfuranyl radicals [7] as well as for radical substitution at the S-atom of thioethers by thiyl radicals (giving alkyl radicals and a S–S bond) [8] has been reported in studies on gas-phase photochemistry. Within this mechanistic hypothesis, the question arises, whether the species accepting the Me group from the sulfuranyl radical would be a Ni(I) or a Ni(II) form of coenzyme F430. Two corresponding pathways, differing in the occurrence of intermediates with F430 in the Ni(I) and Ni(III) valence state, respectively, are shown in *Scheme 2*.

Earlier work from our laboratory has shown that the pentamethyl ester of coenzyme F430 (F430M, **2**) can be reduced by one electron, and that based on its ESR spectrum, the reduced species is best described as Ni(I)F430M in an essentially square-planar coordination environment [10]. Considering the hypothetical mechanisms addressed above, it is of

Scheme 2[a])

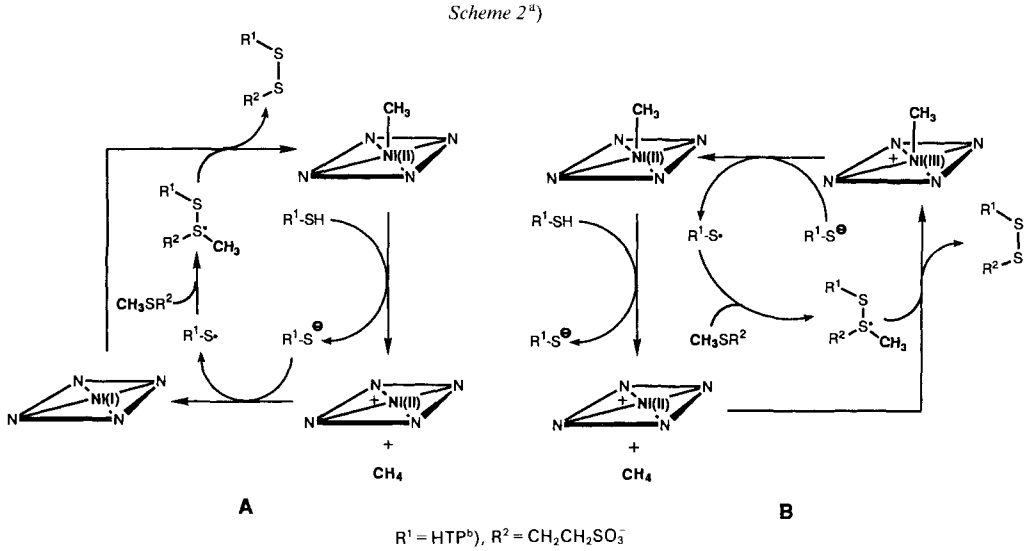

R^1 = HTP[b]), $R^2 = CH_2CH_2SO_3^-$

a) Possible intermediate axial coordination of thiolate to the central nickel atom is not shown.
b) HTP = heptanoyl-*O*-phosphothreonine [9].

interest, whether reversible one-electron oxidation of F430M to a stable product is possible, and whether it would lead to a Ni(III) species or a π-cation radical as observed for some nickel hydroporphyrins [11]. The subject of this communication is oxidative electrochemistry of F430M and the characterization of the one-electron oxidation product by UV/VIS and ESR spectroscopy.

2. Oxidative Electrochemistry of F430M. – In MeCN, with 0.1M $Bu_4N^+BF_4^-$ as electrolyte, the oxidative cyclic voltammogram of F430M (**2**) at a Pt electrode consists of a single, chemically reversible oxidation wave at +0.825 V *vs.* Fc^+/Fc[1]) (*Fig. 1*). The electroanalytical data in the *Table* show deviations from ideal reversible behavior at higher scan rates, indicating quasi-reversibility due to slow heterogeneous electron transfer. Peak separations measured at low scan rates are consistent with a one-electron oxidation, which was confirmed by coulometric determination during bulk electrolysis. To investigate the influence of potential ligands on the half-wave potential, a series of measurements with increasing concentrations of pyridine, imidazole, Bu_4NCl, Bu_4NBr, KCN, KSCN, and anhydrous Bu_4NF was performed. Although cathodic shifts of the

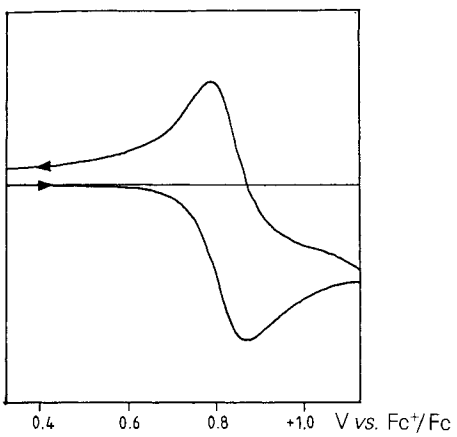

Fig. 1. *Cyclic voltammogram of F430M in MeCN, 0.1M $Bu_4N^+BF_4^-$* (c = 1 mM, T = 24°C, v = 0.05 V/s)

Table. *Oxidative Cyclic Voltammetry Data of F430M* ($c = 1 \times 10^{-3}$ M in MeCN, 0.1M $Bu_4N^+BF_4^-$, T = 25°, Pt electrode). $E_{1/2}$ (0.05 V/s) = +0.825 ● 0.03 V *vs.* Fc^+/Fc.

v [V/s]	ΔE_p [V]	i_{pa}/i_{pc}	$i_{pa}/v^{1/2}$
0.05	0.062	1.04	1.00 (= def)
0.10	0.068	1.10	1.02
0.20	0.076	1.11	1.00
0.40	0.084	1.14	0.97
0.80	0.099	1.08	0.89
1.6	0.128	1.07	0.99
3.2	0.166	1.10	0.95
6.4	0.198	1.09	0.93

[1]) All potential data are referred to the ferricenium/ferrocene couple [12]. Estimated potential *vs.* NHE: *ca.* + 0.625 V.

peak potential were observed, reversibility was lost completely or partially (pyridine, imidazole, Bu_4NCl) in all cases examined[2]). With pyridine (10 equiv. based on F430M), for example, the oxidative peak potential was shifted by −0.25 V, while *ca.* 25% of the reductive peak current was retained at 1.0 V/s.

Bulk electrolysis at +0.9 V *vs.* Fc^+/Fc in a normal H-shaped electrolysis cell, followed by re-reduction at +0 V and mildly acidic aqueous workup, gave 5–10% of 12, 13-didehydro-F430M [1e] as the only side product. In a microcell with a very large electrode surface, allowing complete oxidation within 3 to 5 min, F430M was recovered to > 98% (UV).

3. Electronic Absorption Spectrum of the Oxidation Product. – *Fig. 2* shows the overlap of UV/VIS spectra measured in an optical thin-layer electrolysis cell during stepwise oxidation of F430M. The main absorptions of F430M at 274 and 439 nm disappear and are replaced by a strong absorption of the oxidation product at 368 nm and very weak bands at 595, 890, and 1020 nm[3]). The isosbestic points at 301 and 405 nm

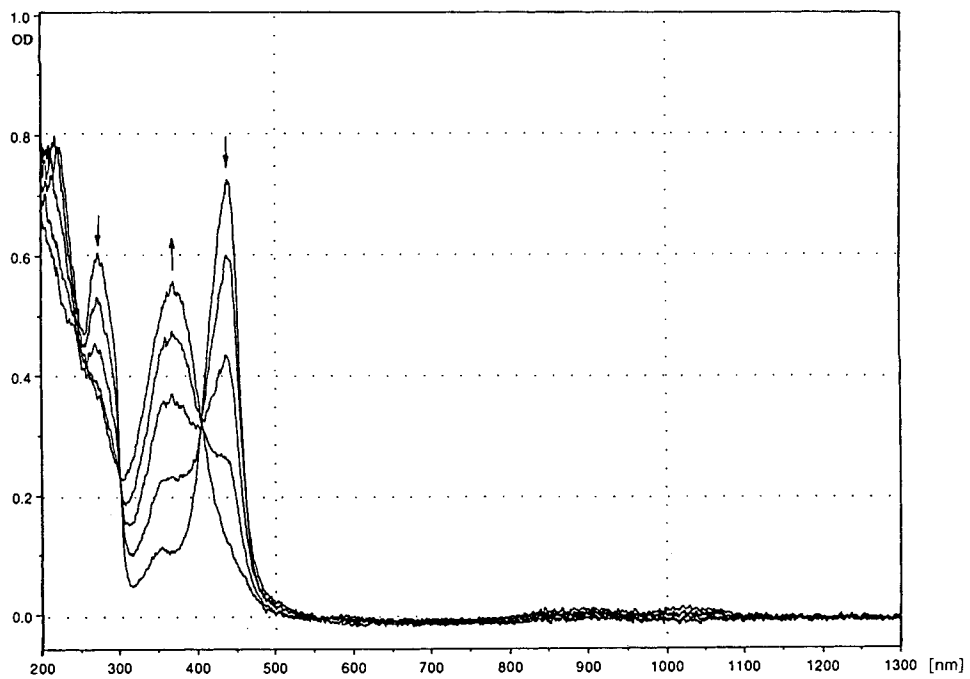

Fig. 2. *Electronic absorption spectra of F430M at various degrees of electrolytic oxidation* (conditions: see *Exper. Part*)

[2]) Bu_4NBr, KSCN, and KCN were clearly oxidized directly at the electrode at lower potentials than F430M. With chloride, fluoride, and pyridine two new reduction waves at −1.00 and −1.53 V, previously assigned to 12,13-didehydro-F430M [1e], appeared on the reverse sweep. This indicates that Cl^-, F^-, and pyridine act as bases inducing dehydrogenation in ring C *via* deprotonation of the primary oxidation product.

[3]) Within experimental error, the extinction of the three week bands was proportional to that of the main band at 368 nm with the same ratio in different experiments. However, in view of the large difference in extinction coefficients and the high noise in the near-IR region, the assignment of these absorptions to Ni(III)F430M has to be considered as tentative.

demonstrate that oxidation leads to a single, stable product. After reduction of the fully oxidized species at −0.3 V *vs.* Fc^+/Fc, the spectrum of Ni(II)F430M was recovered with more than 95% of its original extinction.

4. ESR Spectrum of the Oxidation Product. – The ESR spectrum, obtained from frozen solutions after complete electrolytical oxidation is shown in *Fig. 3*. The strongly anisotropic, nearly axial signal with $g_{\parallel} = 2.020$ and $g_{\perp} = 2.211$ is consistent with a species of effective spin $S = ½$ in which spin density resides predominantly in the d_{z^2} orbital of the central nickel ion. As in the case of reduction to the Ni(I) form, oxidation of F430M is metal-centered, and it leads to a species which is best described as Ni(III)F430M. While

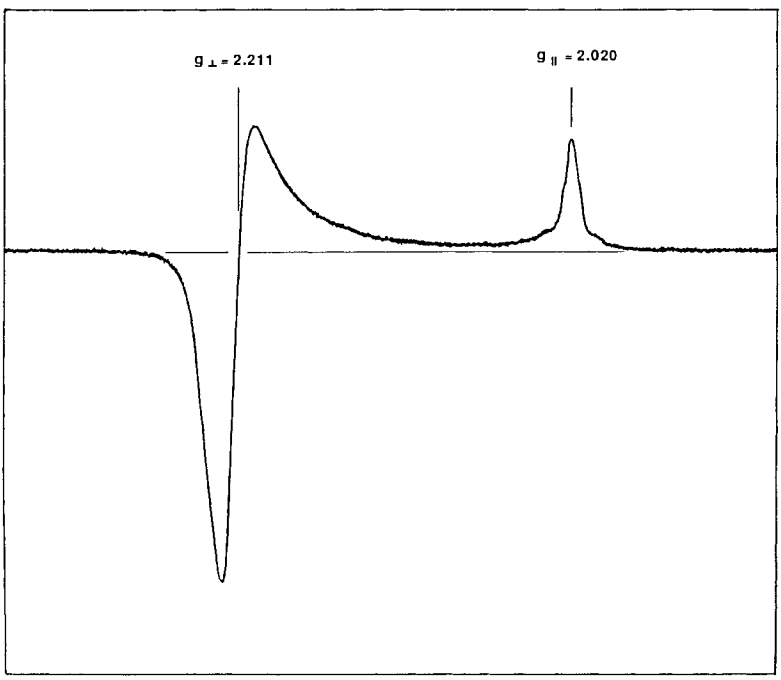

Fig. 3. *ESR spectrum of Ni(III)F430M in frozen MeCN, 0.1 M* $Bu_4N^+BF_4^-$. Conditions: $c = 5 \times 10^{-4}$ M, $T = 98°$ K, modulation amplitude = 2 G, MW power = 2 mW, modulation frequency = 100 kHz, MW frequency = 9.16 GHz.

no hyperfine splitting could be resolved on the $g_{\perp}$ component even at very low modulation amplitude, the $g_{\parallel}$ line shows partially resolved symmetrical shoulders possibly due to hyperfine coupling with the N-atoms of axially coordinated MeCN. The strong anisotropy and the order of the g values indicate, that in MeCN, 0.1 N $Bu_4N^+BF_4^-$, the nickel ion of Ni(III)F430M is in a nearly tetragonal coordination environment with a ligand field that is much stronger in the equatorial than in the axial direction.

5. Discussion. – In a comprehensive study of synthetic tetraaza-macrocyclic Ni complexes by *Bush* and coworkers, the charge of the ligand and the size of the ligand hole have been identified as major factors influencing the standard potentials of the Ni(II)/Ni(I)

and the Ni(III)/Ni(II) redox couples [13]. F430M (**2**) is more easily reducible and distinctly more difficult to oxidize than any of the synthetic square planar Ni complexes with mononegative tetraaza-macrocyclic ligands for which both the Ni(I)- and the Ni(III)-valence states have been reported to be accessible [13a] [14]. The preferential stabilization of the lower valent states parallels the pronounced tendency of Ni(II)F430M to coordinate additional ligands in the axial positions, which has been interpreted in terms of an equatorial ligand hole which is larger than the optimal size for low-spin Ni(II) [15]. Axial electrophilicity and the saddle shaped macrocycle deformation by which hydrocorphins achieve ligand-hole contraction are expected to be even more pronounced in square-planar Ni(III)F430M, than in the Ni(II) state [16]. In fact, while Ni(II)F430M is diamagnetic in MeCN, the order of g values ($g_\perp > g_\parallel$)[4]) and the partially resolved hyperfine splitting of the $g_\parallel$ line in the ESR spectrum of Ni(III)F430M point to a *quasi*-tetragonal, axially 'elongated' coordination environment with two solvent molecules in the axial positions. The marked cathodic shift of peak potentials observed in cyclic voltammetry upon addition of pyridine, imidazole, or chloride, all potentially stronger ligands than MeCN, corroborates this interpretation. Since fast irreversible reactions of the oxidation product also shift the peak potentials in the cathodic direction, the partial loss of reversibility precludes a quantitative evaluation of relative binding constants in the two valence states of F430M.

In view of the high oxidation potential of Ni(II)F430M, four-coordinate or axially weakly coordinated forms of Ni(III)F430 are unlikely as intermediates in the biological process. However, axial coordination of a strong donor like 'CH_3^-', giving a methyl-Ni(III)F430 compound similar to that involved in *Scheme 2B* could lower the oxidation potential sufficiently to prevent immediate homolysis into a methyl radical and Ni(II)F430.

If such a species exists (in the sense of corresponding to a minimum on the potential-energy hypersurface), it would nevertheless be expected to be rather electrophilic. Therefore, reduction of hypothetical methyl-Ni(III)F430 by a thiol to give methyl-Ni(II)F430 as formulated in *Scheme 2B* would be consistent with the properties of both Ni(III)-F430M as reported here and methyl-Ni(II)F430M which will be the subject of a separate communication. Whether methyl-Ni(III)F430 exists and is stable enough to be characterized *in vitro* remains to be demonstrated. Based on the properties of the potential intermediates characterized so far, Ni(I)F430M, Ni(III)F430M, and methyl-Ni(II)F430M, neither of the two hypothetical mechanisms presented in *Scheme 2* can be definitely excluded.

The author thanks Prof. *A. Pfaltz* for valuable discussions, Prof. *R. Thauer* (Universität Marburg) for gifts of F430 extracts, Prof. *J.F.M. Oth* (ETH) for use of electrochemistry equipment and PD Dr. *A. Schweiger* (ETH) for access to the ESR instrument. This work was supported by a research grant from ETH-Zürich.

[4]) Axial ESR spectra with the reversed order $g_\parallel > g_\perp$ observed for some Ni(III) complexes with four strong N-donor ligands, have been interpreted in terms of a truly square-planar geometry with the unpaired electron in the d_{xy} orbital [13a] [14].

Experimental Part

F430M (**2**) was prepared and purified according to the procedure in [1c]. Traces of halogenated solvents, which adversely affect reversibility in electrochemistry, were eliminated by threefold precipitation of F430M from THF with dry benzene.

Tetrabutylammonium tetrafluoroborate ($Bu_4N^+BF_4^-$, *Fluka, puriss.*) was recrystallized three times from AcOEt and dried at r.t. for 5 d at 0.1 mbar. Immediately before use, the weighed amount was dried at 60°/10^{-2} mbar overnight, flushed with Ar after cooling and dissolved in MeCN to give a 0.1M stock soln. The electrolyte solns. were handled with gas tight syringes under Ar.

Acetonitrile (*Carlo Erba*, HPLC-grade) was distilled once under Ar over a 2-m refraction column (reflux ratio 10:1), discarding the first and the last fifths of the distillate. Immediately before use, the solvent was passed over columns of basic, acidic, and neutral alumina (*Woelm*, activity *SI*) sequentially. The resulting electrolyte solns. had an electroneutral window from +1.8 to −2.6 V *vs.* Fc^+/Fc.

Bu_4NCl and *Bu_4NBr* (*FLUKA, p.a.*) were dissolved in benzene/CH_2Cl_2 1:1 and evaporated to dryness *in vacuo* three times, followed by drying at 10^{-2} mbar, r.t. for 2 d.

Anh. *Bu_4NF* was prepared by drying the trihydrate (*Fluka, purum*) at 60°/10^{-2} mbar for 10 h.

Pyridine, imidazole, KCN, and *KSCN* were used as purchased (*Fluka*).

Cyclic Voltammetry. Bruker electrochemistry system with digital storage oscilloscope and *x-y* recorder. Home-built 3-electrode microcell with a volume of 0.5 ml. Working electrode: Pt wire, geometric surface $A = 0.9$ mm^2; Ag-AgCl quasi-reference electrode in a *Luggin* capillary; Hg pool counter electrode. The cell was dried at 120°, assembled hot, and flushed with Ar which had been passed over Cu catalyst (BTS, *BASF*) to remove traces of O_2. F430M (typically 0.2–1.0 mg) was weighed, dissolved in 0.5 ml of electrolyte under Ar, and transferred to the cell with a syringe through a septum cap. Before and between voltammograms, a fine stream of Ar was passed through the soln. IR-drop compensation was used throughout. Potentials were calibrated by simultaneous *in situ* measurement of ferricenium/ferrocene and Ni(III)F430M/Ni(II)F430M in 1:4 molar ratios. Studies of the effect of potential ligands were performed by stepwise addition of 0.5M stock solns. of the additive in MeCN, 0.1M $Bu_4N^+BF_4^-$ to give 0.5, 1.0, 2, 10, and 100 equiv. based on F430M in the cell.

Bulk Electrolysis. Amel mod. *549* potentiostat. Configuration *a*) standard H-shaped cell with two fritted glass disks separating working electrode compartment (9.5 ml) and counter electrode compartment; Pt-sheet working electrode ($A = 6$ cm^2), Ag-AgCl quasi-reference electrode and Hg-pool counter electrode. During electrolysis, the current was measured with a *HP-410C* voltammeter, registered on paper, and integrated planimetrically after subtraction of the background current (25 μA initially at +1.0 V *vs.* Fc^+/Fc). 3.5 mg (3.2 μmol) F430M in 8 ml of electrolyte soln. was electrolysed under vigorous magnetic stirring at +1.0 V. The initial current was 200 μA, the total charge transferred, when the current had decayed to less than 2% of the initial current (45 min), was 3.02 μF (86% yield). In this cell, re-reduction at 0.0 V consistently gave only 2.6–3.0 μF. After reduction, the soln. in the working electrode compartment was transferred into a flask containing 10 ml of aq. 0.1M $NaClO_4$/0.01M $HClO_4$ and extracted into 5 ml of CH_2Cl_2. TLC [1c] and UV/VIS confirmed the presence of both F430M and 12,13-didehydro-F430M in ratios between 90:10 and 96:4. Total recovery was between 87% and 93% based on initial F430M. Configuration *b*) Identical procedure in a micro H-cell (0.8 ml) with a very long, finely wound Pt-coil electrode ($A = ca.$ 30 cm^2) filling most of the working-electrode compartment. Convection was achieved by passing a stream of Ar (presaturated with MeCN to prevent a reduction of solvent volume) through the soln. With 3.2 mg F430M (3 μmol) in 0.8 ml electrolyte, the initial current was *ca.* 12 mA. After 6 min (decay of current to 5%), 2.8 μF (93%) of charge had passed, and re-reduction at 0.0 V gave 3.1 μF in 8 min. After workup, less than 2% of 12,13-didehydro-F430M could be detected by UV/VIS.

UV/VIS Spectroscopy in Thin-Layer Electrolysis Cell (Fig. 4). The cell consisted of two plates of suprasil optical quartz, fused along the edges. The optical pathlength was 0.03 cm, the Pt-grid electrode had an optical density of 0.11. An identical cell filled with electrolyte soln. was used in the reference path. Stepwise electrolysis, controlled with an *Amel 549* potentiostat, was performed directly in the UV/VIS spectrometer (*Uvikon Kontron* for 200–900 nm, *Cary 18* with a home-built data station for 200–2000 nm). After stepping up the potential, *Nernst* equilibrium was reached within 30 to 40 s, and the UV/VIS spectrum was measured with constant potential applied to the electrodes. UV of Ni(III)F430M ($c = 5 \times 10^{-4}$ M, MeCN 0.1M $Bu_4N^+BF_4^-$, 24°): 265 (sh), 303 (6600, min), 368 (15400, max), 554 (< 100, min), 594 (400, max[3]), 700 (< 100, min), 890 (ca 600, max[3]), 970 (*ca.* 200, min[3]), 1020 (*ca.* 650, max[3]).

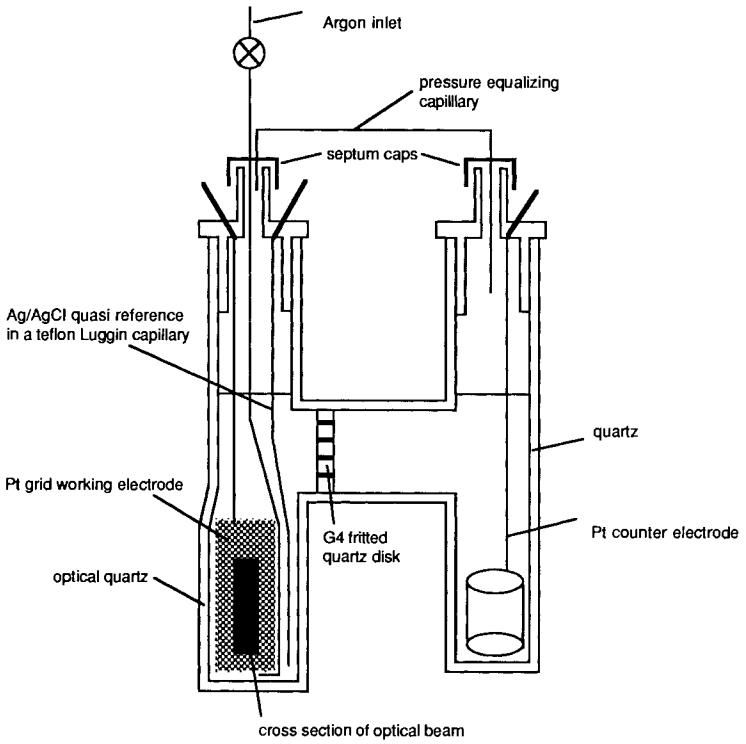

Fig. 4. *Optical thin-layer electrolysis cell*

ESR Spectroscopy. Varian E-Line Century X-band spectrometer with standard TE_{102} cavity and quartz dewar cooled by a stream of cold N_2 gas generated from liquid N_2. Temp. was measured by a *Pt-100* resistance thermometer placed in the cavity immediately before and after the ESR measurement. The g- values were taken as the maximum ($g_{\|}$) and the zero crossing point ($g_{\perp}$), and calibrated against solid DPPH (g = 2.0037) contained in a sealed cap. within the EPR tube. For typical parameters, see caption of *Fig. 3. Sample preparation.* After complete oxidation of F430M in either the H microcell or the optical thin-layer electrolysis cell, *ca.* 300 µl of the soln. was transferred *via* a fine stainless steel cap. to a 4-mm quartz ESR tube closed with a serum cap and filled with O_2-free N_2. After the transfer, the soln. was immediately frozen in liquid N_2.

REFERENCES

[1] a) R.P. Gunsalus, R.S. Wolfe, *FEMS Microbiol. Lett.* **1978,** *3,* 191; b) G. Diekert, B. Klee, R.K. Thauer, *Arch. Microbiol.* **1980,** *124,* 103; c) A. Pfaltz, B. Jaun, A. Fässler, A. Eschenmoser, R. Jaenchen, H.H. Gilles, G. Diekert, R.K. Thauer, *Helv. Chim. Acta* **1982,** *65,* 828; d) D.A. Livingston, A. Pfaltz, J. Schreiber, A. Eschenmoser, D. Ankel-Fuchs, J. Moll, R. Jaenchen, R.K. Thauer, *ibid.* **1984,** *67,* 334; e) A. Pfaltz, D.A. Livingston, B. Jaun, G. Diekert, R.K. Thauer, A. Eschenmoser, *ibid.* **1985,** *68,* 1338; f) J.R. Lancaster, Jr., Ed., 'The Bioinorganic Chemistry of Nickel', VCH Publishers, New York, 1988, pp. 275–298.

[2] a) W.L. Ellefson, R.S. Wolfe, *J. Biol. Chem.* **1980,** *255,* 8388; *ibid.* **1981,** *256,* 4259.

[3] a) J. Ellermann, S. Rospert, R.K. Thauer, M. Bokranz, A. Klein, M. Voges, A. Berkessel, *Eur. J. Biochem.* **1989,** *184,* 63; b) W.L. Ellefson, W.B. Whitman, R.S. Wolfe, *Proc. Natl. Acad. Sci. U.S.A.* **1982,** *79,* 3707; c) K.M. Noll, K.L. Rinehardt, Jr., R.S. Tanner, R.S. Wolfe, *ibid.* **1986,** *83,* 4238; d) K.M. Noll,

M.I. Donelly, R.S. Wolfe, *J. Biol. Chem.* **1987,** *262,* 513; e) A. Kobelt, A. Pfaltz, D. Ankel-Fuchs, R.K. Thauer, *FEBS Lett.* **1987,** *214,* 265; f) T.A. Bobik, K.D. Olson, K.M. Noll, R.S. Wolfe, *Biochem. Biophys. Res. Commun.* **1987,** *149,* 455; g) J. Ellermann, R. Hedderich, R. Böcher, R.K. Thauer, *Eur. J. Biochem.* **1988,** *172,* 669.

[4] G. Färber, W. Keller, Ch. Kratky, B. Jaun, A. Pfaltz, Ch. Spinner, A. Kobelt, A. Eschenmoser, in preparation.

[5] a) S.P.J. Albracht, D. Ankel-Fuchs, R. Böcher, J. Ellermann, J. Moll, J.W. van der Zwaan, R.K. Thauer, *Biochem. Biophys. Acta* **1988,** *955,* 86; b) J.A. Krzycki, R.C. Prince, *ibid.* **1990,** *1015,* 53.

[6] K.M. Noll, K.L. Rinehart, Jr., R.S. Tanner, R.S. Wolfe, *Proc. Natl. Acad. Sci. U.S.A.* **1986,** *83,* 4238.

[7] E. Anklam, S. Steenken, *J. Photochem. A* **1988,** *43,* 233.

[8] T. Yokota, O.P. Strausz, *J. Phys. Chem.* **1979,** *83,* 3196.

[9] P. van Beelen, A.P.M. Stassen, J.W.G. Bosch, G.D. Vogels, W. Guijt, C.A.G. Haasnoot, *Eur. J. Biochem.* **1984,** *138,* 563; J.C. Escalante-Semerena, J.A. Leigh, K.L. Rinehart, Jr., R.S. Wolfe, *Proc. Natl. Acad. Sci. U.S.A.* **1984,** *81,* 1976.

[10] B. Jaun, A. Pfaltz, *J. Chem. Soc., Commun.* **1986,** 1327.

[11] G. Gritzner, J. Kuta, *Pure Appl. Chem.* **1984,** *56,* 461.

[12] A.M. Stolzenberg, M.T. Stershic, *Inorg. Chem.* **1988,** *27,* 1614.

[13] a) F.V. Lovecchio, E.S. Gore, D.H. Bush, *J. Am. Chem. Soc.* **1974,** *96,* 3109; b) D.H. Bush, *Acc. Chem. Res.* **1978,** *11,* 392.

[14] A.G. Lippin, A. McAuley, *Adv. Inorg. Chem.* **1988,** *32,* 241, and ref. cit. therein.

[15] A. Eschenmoser, *Ann. N.Y. Acad. Sci.* **1986,** *471,* 108.

[16] a) C. Kratky, R. Waditschatka, C. Angst, J.E. Johansen, J.C. Plaquevent, J. Schreiber, A. Eschenmoser, *Helv. Chim. Acta* **1985,** *68,* 1312; b) R. Waditschatka, C. Kratky, B. Jaun, J. Heinzer, A. Eschenmoser, *J. Chem. Soc., Chem. Commun.* **1985,** 1604; c) C. Kratky, A. Fässler, A. Pfaltz, B. Kräutler, B. Jaun, A. Eschenmoser, *ibid.* **1984,** 1368.